

Neutrino Mass, Dark Matter and Baryon Asymmetry without Lepton Number Violation

Shinya Kanemura,^{1,*} Kodai Sakurai,^{2,†} and Hiroaki Sugiyama^{3,‡}

¹*Department of Physics, Osaka University, Toyonaka, Osaka 560-0043, Japan*

²*Department of Physics, University of Toyama,
3190 Gofuku, Toyama 930-8555, Japan*

³*Liberal Arts and Sciences, Toyama Prefectural University, Toyama 939-0398, Japan*

Abstract

We propose a model to explain tiny masses of neutrinos with the lepton number conservation, where neither too heavy particles beyond the TeV-scale nor tiny coupling constants are required. Assignments of conserving lepton numbers to new fields result in an unbroken Z_2 symmetry that stabilizes the dark matter candidate (the lightest Z_2 -odd particle). In this model, Z_2 -odd particles play an important role to generate the mass of neutrinos. The scalar dark matter in our model can satisfy constraints on the dark matter abundance and those from direct searches. It is also shown that the strong first-order phase transition, which is required for the electroweak baryogenesis, can be realized in our model. In addition, the scalar potential can in principle contain CP-violating phases, which can also be utilized for the baryogenesis. Therefore, three problems in the standard model, namely absence of neutrino masses, the dark matter candidate, and the mechanism to generate baryon asymmetry of the Universe, may be simultaneously resolved at the TeV-scale. Phenomenology of this model is also discussed briefly.

* kanemu@het.phys.sci.osaka-u.ac.jp

† sakurai@jodo.sci.u-toyama.ac.jp

‡ shiro324@gmail.com

I. INTRODUCTION

The standard model (SM) of particle physics was established by the discovery of a Higgs boson at the CERN large hadron collider (LHC) [1]. This does not mean that theoretical particle physics has been completed because several problems remain in the high energy physics. For example, neutrinos are massless in the SM while the discovery of neutrino oscillations [2] is the evidence of tiny neutrino masses. The absence of the candidate for the dark matter in the SM, which accounts for 27% of the Universe [3], must be resolved. The baryon asymmetry of the Universe cannot be explained in the SM, so that the SM must be extended to include a mechanism to generate the baryon asymmetry of the Universe.

Reasons why neutrinos are massless in the SM are the absence of right-handed neutrinos ν_R and the lepton number conservation. If we introduce ν_R to the SM, neutrino masses can be generated via the naive Yukawa interaction with the Higgs doublet field in the SM similarly to masses of quarks and charged leptons. However, the Yukawa coupling constant seems to be unnaturally small ($\lesssim 10^{-12}$). Instead of such fine-tuned coupling constants, in the (type-I) seesaw mechanism [4] very large Majorana masses of ν_R are introduced with the lepton number violation for a natural realization of tiny neutrino masses. Such heavy Majorana neutrinos can also be used for leptogenesis [5] to explain the baryon asymmetry of the Universe.

There is an alternative scenario, in which the smallness of neutrino masses can be explained by the quantum effect. For example, tiny Majorana masses are radiatively generated at the one-loop level in the Ma model [6], where new particles are not necessarily very heavy and can be in the TeV-scale. Hence, scenarios along this line can be in principle tested directly by collider experiments. In addition, new particles that are involved in the one-loop diagram include the dark matter candidate. Similarly to the Ma model, the Aoki-Kanemura-Seto (AKS) model [7] gives tiny Majorana neutrino masses at the three-loop level, where the dark matter candidate contributes to the three-loop diagram. One of the remarkable features of this model is that two $SU(2)_L$ -doublet Higgs fields are required. In general two Higgs doublet models can contain CP violating phases in the Higgs sector. It is shown that the strong first-order phase transition is realized in the AKS model which is required for successful electroweak baryogenesis [8]. Thus, three problems can be simultaneously resolved at the TeV-scale in the AKS model, which can be probed at collider experiments.

In Refs. [9, 10], models for generating the neutrino mass matrix are classified into several groups by focusing on combinations of Yukawa matrices in the mass matrix. In the systematic study for the Majorana neutrino mass generation [9], no combination other than the one in the AKS model involves simultaneously the dark matter candidate and the second $SU(2)_L$ -doublet Higgs field that has the vacuum expectation value. On the other hand, it was found in Ref. [10] that masses of Dirac neutrinos can be radiatively generated by using the dark matter candidate and the second $SU(2)_L$ -doublet Higgs field (See Figs. 11, 13 and 15 in Ref. [10]).

In this letter, we propose a concrete model, where the combination of Yukawa matrices to generate Dirac neutrino mass matrix corresponds to the structure in Fig. 15 in Ref. [10]. As the lepton number violating phenomena such as the neutrinoless double beta decay have not been observed up to now, it would be important to consider the possibility that neutrinos are purely of the Dirac type fermions, whose masses conserve the lepton number. Along this line, we investigate the new model to simultaneously provide the origin of tiny neutrino masses, the dark matter candidate, and the source of the baryon asymmetry of the Universe. We here ignore the CP violation in the scalar potential for simplicity and concentrate on the realization of the strong first-order phase transition, which is necessary for successful electroweak baryogenesis. Calculation for the baryon asymmetry with the CP violation is beyond the scope of this letter, and leave it as our future work.

This letter is organized as follows. In Sec. II, we present our model where Dirac neutrino masses are generated at the one-loop level. We see that our model can be consistent with neutrino oscillation data and the relic abundance of the dark matter as well as the strong first-order electroweak phase transition required for the electroweak baryogenesis scenario. Section III is devoted to further phenomenological studies such as lepton flavor violating decays of charged leptons, the spin-independent scattering cross section of the dark matter on a proton, and collider phenomenology. Conclusions are shown in Sec. IV. Some formulae are presented in Appendix.

	Z_2 -even					Z_2 -odd		
	ℓ_R	ν_R	Φ_1	Φ_2	s_3^+	ψ_R^0	s_2^0	s_2^+
Spin	1/2	1/2	0	0	0	1/2	0	0
$SU(2)_L$	<u>1</u>	<u>1</u>	<u>2</u>	<u>2</u>	<u>1</u>	<u>1</u>	<u>1</u>	<u>1</u>
$U(1)_Y$	-1	0	1/2	1/2	1	0	0	1
Lepton Number	1	1	0	0	0	0	-1	-1
Z'_2	Even	Odd	Even	Even		Even	Odd	Even
Z''_2	Odd	Even	Odd	Even	Odd	Even	Even	Odd

TABLE I. The list of new fields in our model, which are added to the SM. A scalar field s_3^+ can be both of even and odd for the Z'_2 symmetry.

II. THE MODEL

A. Particle contents and Lagrangian

In our model, the lepton number (L) conservation is imposed¹. We introduce gauge singlet fermions ν_{iR} ($i = 1-3$) with $L = 1$, which result in right-handed components of Dirac neutrinos. New fields that are introduced to the SM are listed in Table I. Fermions ψ_{aR}^0 ($a = 1-3$) are also gauge singlet though they have $L = 0$ in comparison with $L = 1$ for ν_R . This model involves two $SU(2)_L$ -doublet scalar fields $\Phi_1 \equiv (\phi_1^+, (v_1 + \phi_{1r}^0 + i\phi_{1i}^0)/\sqrt{2})^T$ and $\Phi_2 \equiv (\phi_2^+, (v_2 + \phi_{2r}^0 + i\phi_{2i}^0)/\sqrt{2})^T$ with $Y = 1/2$ and $L = 0$, where $v^2 = v_1^2 + v_2^2 = (246 \text{ GeV})^2$. Scalar fields s_2^+ and s_3^+ are $SU(2)_L$ -singlet with $Y = 1$; the former has $L = -1$ while the latter does $L = 0$. The complex scalar field s_2^0 is a gauge singlet with $L = -1$.

If the Dirac neutrino mass is simply generated via the Yukawa interaction $y_\nu \bar{L} \tilde{\Phi} \nu_R$, where $\tilde{\Phi} \equiv \epsilon \Phi^*$, the size of the Yukawa coupling constant is extremely small ($y_\nu \sim 10^{-12}$), which seems to be unnatural and cannot be experimentally tested. In our model, the Yukawa interaction is forbidden at the tree-level by imposing a softly broken Z_2 symmetry (we refer to it as the Z'_2 symmetry), under which ν_R is odd while $SU(2)_L$ -doublet lepton and scalars are even. Properties of additional particles with respect to the Z'_2 are also shown in Table I. The scalar field s_3^+ can be both of even and odd. The Z'_2 is softly broken in the scalar

¹ The spharelon process breaks $B + L$ at the finite temperature, where B denotes the baryon number. The process is utilized for the electroweak baryogenesis scenario.

potential, and then the Dirac neutrino mass can be generated at the two-loop level as we see later.

Relevant parts of Yukawa interactions for generating neutrino masses are given by

$$\mathcal{L}_{\text{Yukawa}} = y_\ell \overline{L}_\ell \Phi_1 \ell_R + (Y_\psi^+)_{\ell a} \overline{(\ell_R)^c} \psi_{aR}^0 s_2^+ + (Y_\psi^0)_{ia} \overline{(\nu_{iR})^c} \psi_{aR}^0 s_2^0 + \text{h.c.} \quad (1)$$

In order to forbid the flavor changing neutral current (FCNC) at the tree level, we impose another softly-broken Z_2 symmetry (we represent it as Z_2'') as shown in Table. I. Quarks and the lepton doublet field are Z_2'' -even. Then, ℓ_R has the Yukawa interaction only with Φ_1 similarly to the the type-X two Higgs doublet model [11] (see also Refs. [12–14]).

The scalar potential is given by

$$\begin{aligned} V = & V_{\text{THDM}} + m_{s_0}^2 |s_2^0|^2 + m_{s_2}^2 |s_2^+|^2 + m_{s_3}^2 |s_3^+|^2 \\ & + \left(\mu_3 \left[\Phi_2^\dagger \epsilon \Phi_1^* s_3^+ \right] + \text{h.c.} \right) + \left(\mu'_3 \left[s_3^- s_2^+ s_2^{0*} \right] + \text{h.c.} \right) \\ & + \lambda_{s_0 s_2} |s_2^0|^2 |s_2^+|^2 + \lambda_{s_0 s_3} |s_2^0|^2 |s_3^+|^2 + \lambda_{s_2 s_3} |s_2^+|^2 |s_3^+|^2 \\ & + \lambda_{\phi_1 s_0} \Phi_1^\dagger \Phi_1 |s_2^0|^2 + \lambda_{\phi_1 s_2} \Phi_1^\dagger \Phi_1 |s_2^+|^2 + \lambda_{\phi_1 s_3} \Phi_1^\dagger \Phi_1 |s_3^+|^2 \\ & + \lambda_{\phi_2 s_0} \Phi_2^\dagger \Phi_2 |s_2^0|^2 + \lambda_{\phi_2 s_2} \Phi_2^\dagger \Phi_2 |s_2^+|^2 + \lambda_{\phi_2 s_3} \Phi_2^\dagger \Phi_2 |s_3^+|^2 \\ & + \lambda_{s_0} |s_2^0|^4 + \lambda_{s_2} |s_2^+|^4 + \lambda_{s_3} |s_3^+|^4, \end{aligned} \quad (2)$$

where V_{THDM} is the following one in two Higgs double models without the tree-level FCNC:

$$\begin{aligned} V_{\text{THDM}} = & m_{11}^2 \Phi_1^\dagger \Phi_1 + m_{22}^2 \Phi_2^\dagger \Phi_2 - \left(m_{12}^2 \Phi_1^\dagger \Phi_2 + \text{h.c.} \right) \\ & + \frac{\lambda_1}{2} (\Phi_1^\dagger \Phi_1)^2 + \frac{\lambda_2}{2} (\Phi_2^\dagger \Phi_2)^2 + \lambda_3 (\Phi_1^\dagger \Phi_1) (\Phi_2^\dagger \Phi_2) \\ & + \lambda_4 (\Phi_1^\dagger \Phi_2) (\Phi_2^\dagger \Phi_1) + \left(\frac{\lambda_5}{2} (\Phi_1^\dagger \Phi_2)^2 + \text{h.c.} \right). \end{aligned} \quad (3)$$

The complex phases of μ_3 , μ'_3 , and λ_5 can be eliminated by the rephasing of s_3^+ , s_2^+ (or s^0), and Φ_1 (or Φ_2), respectively. For simplicity in this letter, we take m_{12}^2 as a real parameter and also assume that the CP is not spontaneously violated. Z_2' and Z_2'' symmetries are softly broken by $\mu_3 \mu'_3$ and m_{12}^2 , respectively.

By virtue of the assignments of conserved lepton numbers to new fields, there appears an unbroken Z_2 symmetry such that ψ_R^0 , s_2^0 , and s_2^+ have the odd parity. The Z_2 symmetry can be utilized for the stabilization of the dark matter candidate.

Z_2 -odd scalar fields s_2^0 and s_2^+ are mass eigenstates \mathcal{H}^0 and \mathcal{H}^+ without mixings with other fields, respectively. Their masses are calculated as

$$m_{\mathcal{H}^0}^2 = m_{s_0}^2 + \frac{\lambda_{\phi_1 s_0} v_1^2}{2} + \frac{\lambda_{\phi_2 s_0} v_2^2}{2}, \quad (4)$$

$$m_{H^+}^2 = m_{s_2}^2 + \frac{\lambda_{\phi_1 s_2} v_1^2}{2} + \frac{\lambda_{\phi_2 s_2} v_2^2}{2}. \quad (5)$$

Three Z_2 -even charged scalar fields (ϕ_1^+ , ϕ_2^+ , and s_3^+) result in three mass eigenstates (H_1^+ , H_2^+ , and the Nambu-Goldstone boson G^+) as

$$\begin{pmatrix} G^+ \\ H_1^+ \\ H_2^+ \end{pmatrix} = \begin{pmatrix} \cos \beta & \sin \beta & 0 \\ -\sin \beta \cos \theta_+ & \cos \beta \cos \theta_+ & \sin \theta_+ \\ \sin \beta \sin \theta_+ & -\cos \beta \sin \theta_+ & \cos \theta_+ \end{pmatrix} \begin{pmatrix} \phi_1^+ \\ \phi_2^+ \\ s_3^+ \end{pmatrix}, \quad (6)$$

where $\tan \beta = v_2/v_1$. The mixing angle θ_+ can be expressed as

$$\tan(2\theta_+) = \frac{-2(M_{H^+}^{\prime 2})_{12}}{(M_{H^+}^{\prime 2})_{22} - (M_{H^+}^{\prime 2})_{11}}, \quad (7)$$

where the 2×2 matrix $M_{H^+}^{\prime 2}$ is defined as

$$M_{H^+}^{\prime 2} \equiv \begin{pmatrix} \frac{v^2}{v_1 v_2} m_{12}^2 - \frac{1}{2}(\lambda_4 + \lambda_5)v^2 & \frac{v\mu_3}{\sqrt{2}} \\ \frac{v\mu_3}{\sqrt{2}} & m_{s_3}^2 + \frac{\lambda_{\phi_1 s_3} v_1^2}{2} + \frac{\lambda_{\phi_2 s_3} v_2^2}{2} \end{pmatrix}. \quad (8)$$

Masses of H_1^+ and H_2^+ are given by

$$m_{H_1^+}^2 = \frac{1}{2} \left\{ (M_{H^+}^{\prime 2})_{11} + (M_{H^+}^{\prime 2})_{22} - \sqrt{((M_{H^+}^{\prime 2})_{22} - (M_{H^+}^{\prime 2})_{11})^2 + 4(M_{H^+}^{\prime 2})_{12}^2} \right\}, \quad (9)$$

$$m_{H_2^+}^2 = \frac{1}{2} \left\{ (M_{H^+}^{\prime 2})_{11} + (M_{H^+}^{\prime 2})_{22} + \sqrt{((M_{H^+}^{\prime 2})_{22} - (M_{H^+}^{\prime 2})_{11})^2 + 4(M_{H^+}^{\prime 2})_{12}^2} \right\}. \quad (10)$$

Z_2 -even neutral scalars (CP-even h and H , CP-odd A , and the Nambu-Goldstone boson G^0) are constructed from Φ_1 and Φ_2 similarly to two Higgs doublet models, where h is the discovered Higgs boson with the mass $m_h = 125$ GeV. Throughout this letter, we take $\sin(\beta - \alpha) = 1$, where α denotes the mixing angle between ϕ_{1r}^0 and ϕ_{2r}^0 .

Differences of our model from the AKS model are as follows.

- i) Neutrinos are Dirac fermions, for which right-handed neutrinos ν_R are introduced with the lepton number conservation, while the AKS model is for Majorana neutrino masses without ν_R .
- ii) Assignments of conserving lepton numbers to new fields stabilize the dark matter candidate instead of the imposed Z_2 symmetry in the AKS model.
- iii) The Z_2 -odd neutral scalar s_2^0 is a complex field with the conserved lepton number while the AKS model involves a Z_2 -odd real scalar field.
- iv) The Z_2 -even $SU(2)_L$ -singlet charged scalar s_3^+ is introduced, which is absent in the AKS model.

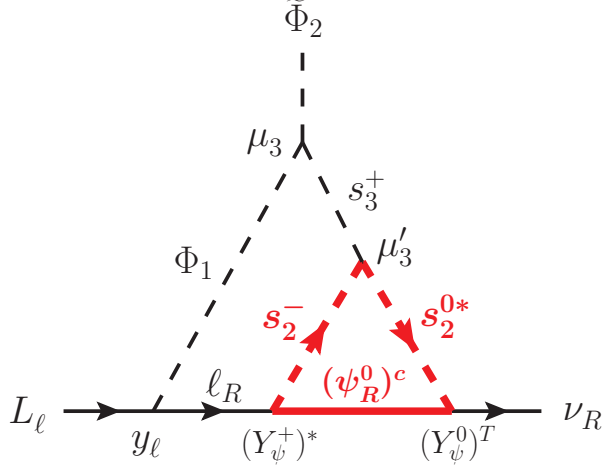


FIG. 1. The diagram for generating Dirac neutrino masses in our model. The arrow shows the flow of the lepton number, which is conserved in our model.

B. Dirac Neutrino Masses

Neutrinos acquire Dirac masses at the two-loop level as $(m_D)_{\ell i} \overline{\nu_{\ell L}} \nu_{iR}$ via the diagram in Fig. 1. Notice that the interaction $\Phi_2^\dagger \epsilon \Phi_1^* s_2^+ s_2^0$ is forbidden because this is a hard breaking term of Z'_2 . The coupling constant μ_3 can be expressed by θ_+ . Although arbitrary number of $|\Phi_i|^2$ can be attached to each of scalar lines in the diagram with appropriate coupling constant λ , such effects to neutrino masses are involved in scalar mass eigenvalues as λv_i^2 . As a result, the mass matrix $(m_D)_{\ell i}$ is given by

$$(m_D)_{\ell i} = \frac{1}{\sqrt{2}v} m_\ell \left(m_{H_2^+}^2 - m_{H_1^+}^2 \right) \mu_3' \tan \beta \sin(2\theta_+) \sum_a (Y_\psi^+)_{\ell a}^* (Y_\psi^0)_{ai}^T I_{\ell a}, \quad (11)$$

where the explicit formula for the two-loop function $I_{\ell a}$ is presented in Appendix A. We can take the basis where ν_{iR} are already mass eigenstates without loss of generality. Then, the mass matrix can be expressed as $m_D = U_{\text{MNS}} \text{diag}(m_1, m_2, m_3)$ with neutrino mass eigenvalues m_i ($i = 1-3$). The Maki-Nakagawa-Sakata matrix [15] U_{MNS} can be parametrized as

$$U_{\text{MNS}} = \begin{pmatrix} 1 & 0 & 0 \\ 0 & c_{23} & s_{23} \\ 0 & -s_{23} & c_{23} \end{pmatrix} \begin{pmatrix} c_{13} & 0 & s_{13}e^{-i\delta} \\ 0 & 1 & 0 \\ -s_{13}e^{i\delta} & 0 & c_{13} \end{pmatrix} \begin{pmatrix} c_{12} & s_{12} & 0 \\ -s_{12} & c_{12} & 0 \\ 0 & 0 & 1 \end{pmatrix}, \quad (12)$$

where $c_{ij} \equiv \cos \theta_{ij}$ and $s_{ij} \equiv \sin \theta_{ij}$. Neutrino oscillation data result in We take the following values consistent with neutrino oscillation data:

$$\sin^2 \theta_{23} = 0.514 [16], \quad \sin^2(2\theta_{13}) = 0.0841 [17], \quad \tan^2 \theta_{12} = 0.427 [18], \quad (13)$$

$$\Delta m_{32}^2 = 2.51 \times 10^{-3} \text{ eV}^2 [16], \quad \Delta m_{21}^2 = 7.46 \times 10^{-5} \text{ eV}^2 [18], \quad (14)$$

where $\Delta m_{ij}^2 \equiv m_i^2 - m_j^2$. For example, m_{D} for these values with $m_3 > m_1 = 0.01 \text{ eV}$ and $\delta = 0$ can be generated in our model by the following benchmark set of parameter values:

$$Y_{\psi}^+ = \begin{pmatrix} 1 & 0.01 & 0.01 \\ 0.01 & 1 & 0.01 \\ 0.01 & 0.01 & 1 \end{pmatrix}, \quad Y_{\psi}^0 \simeq \begin{pmatrix} 3.2 \times 10^{-1} & -4.0 \times 10^{-3} & -3.1 \times 10^{-3} \\ 2.7 \times 10^{-1} & -1.4 \times 10^{-3} & -2.8 \times 10^{-3} \\ 2.9 \times 10^{-1} & 3.9 \times 10^{-3} & -2.6 \times 10^{-3} \end{pmatrix}, \quad (15)$$

$$\mu'_3 = 50 \text{ GeV}, \quad \tan \beta = 3, \quad \sin \theta_+ = 0.1,$$

$$m_{H_1^+} = 200 \text{ GeV}, \quad m_{H_2^+} = 300 \text{ GeV}, \quad m_{\mathcal{H}^+} = 350 \text{ GeV}, \quad m_{\mathcal{H}^0} = 63 \text{ GeV},$$

$$m_{\psi_{1R}} = m_{\psi_{2R}} = m_{\psi_{3R}} = 5 \text{ TeV}.$$

We see that tiny Dirac neutrino masses are obtained without extremely small values of parameters and very heavy particles. Notice that \mathcal{H}^0 for the benchmark set is the lightest Z_2 -odd particle and the dark matter candidate.

For different values of parameters, one of ψ_{iR}^0 can be the lightest Z_2 -odd particle and the dark matter candidate.

C. Relic Abundance of the Dark Matter

For the benchmark set in eq. (15), the dark matter candidate (the lightest Z_2 -odd particle) is a complex scalar particle \mathcal{H}^0 . Its relic abundance ($\Omega_{\mathcal{H}^0} h^2 + \Omega_{\mathcal{H}^{0*}} h^2 \simeq 2\Omega_{\mathcal{H}^0} h^2$) must be consistent with the experimental constraint $\Omega_{\text{DM}} h^2 = 0.1186 \pm 0.0020$ [3]. Figures 2 and 3 show diagrams of pair and self-annihilation of \mathcal{H}^0 , respectively². See Appendix B for formulae of cross sections for them. The cross section σ , which is the sum of cross sections for these annihilation processes, can be expanded as $\sigma v_{\text{rel}} \simeq \sigma_0 + \sigma_1 v_{\text{rel}}^2$ with respect to the relative velocity v_{rel} between initial particles. Then, the relic abundance of \mathcal{H}^0 can be

² Contribution of $\mathcal{H}^0 \mathcal{H}^{0*} \rightarrow h(H) \rightarrow \gamma\gamma$ is always subdominant while loop diagrams for $\mathcal{H}^0 \mathcal{H}^{0*} \rightarrow \gamma\gamma$ in Fig. 2 can be dominant ones in some parameter region.

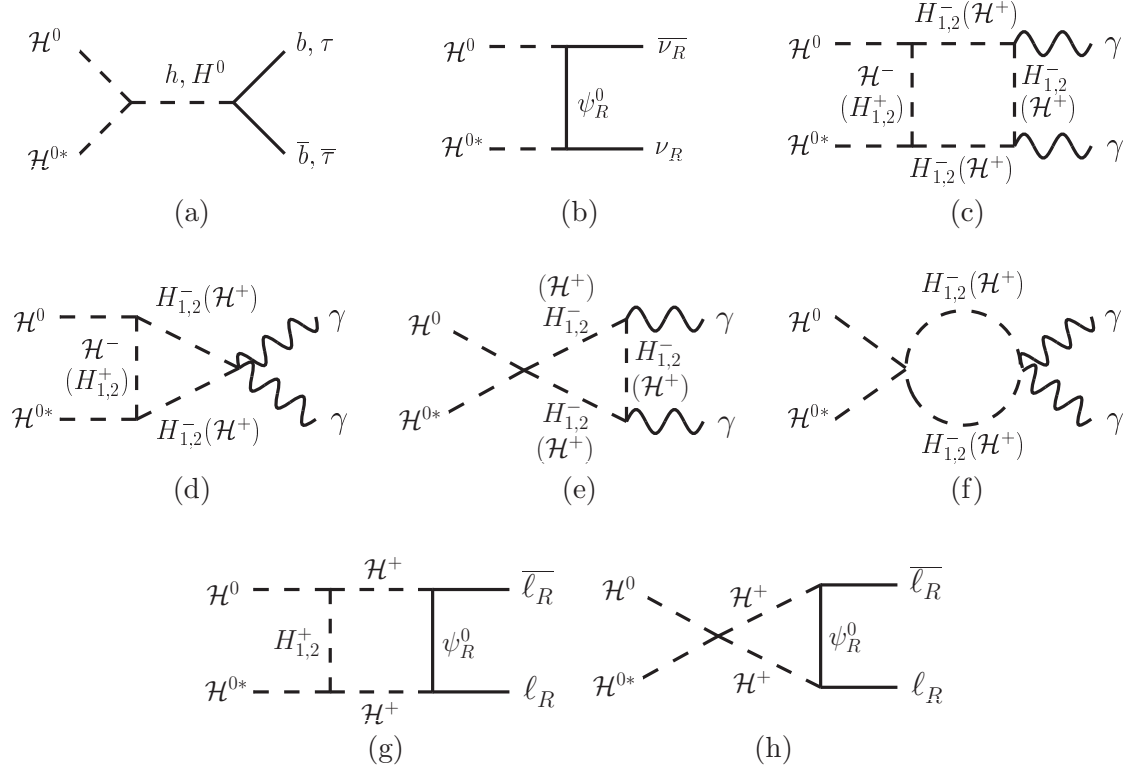


FIG. 2. Diagrams of the pair-annihilation of \mathcal{H}^0 .

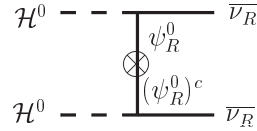


FIG. 3. The diagram of the self-annihilation of \mathcal{H}^0 .

calculated [19] with

$$\Omega_{\mathcal{H}^0} h^2 = 1.04 \times 10^9 \frac{\sqrt{g_*}}{g_{*S}} \frac{\text{GeV}}{m_{\text{Pl}}} \frac{\text{GeV}^{-2}}{\sigma_0} x_f \left(1 + \frac{3\sigma_1}{\sigma_0} x_f^{-1} \right)^{-1}, \quad (16)$$

$$x_f = \ln \left[0.038 \frac{g_{\mathcal{H}^0}}{\sqrt{g_*}} m_{\text{Pl}} m_{\mathcal{H}^0} \sigma_0 \right] - \frac{1}{2} \ln \left[\left\{ 0.038 \frac{g_{\mathcal{H}^0}}{\sqrt{g_*}} m_{\text{Pl}} m_{\mathcal{H}^0} \sigma_0 \right\} \right] + \ln \left[1 + \frac{6\sigma_1}{\sigma_0} \left\{ \ln \left(0.038 \frac{g_{\mathcal{H}^0}}{\sqrt{g_*}} m_{\text{Pl}} m_{\mathcal{H}^0} \sigma_0 \right) \right\}^{-1} \right], \quad (17)$$

where $m_{\text{Pl}} = 1.2 \times 10^{19} \text{ GeV}$ is the Planck mass, $g_* = g_{*S} = 106.75$, and $g_{\mathcal{H}^0} = 1$. Figure 4 is obtained by using the benchmark set in eq. (15) ($m_{\mathcal{H}^0}$ is taken as the x -axis) with

$$m_H = 200 \text{ GeV}, \quad \lambda_{\phi_{1s0}} = 0.02, \quad \lambda_{\phi_{2s0}} = 0.005. \quad (18)$$

We see that the observed value of $\Omega_{\text{DM}} h^2$ (horizontal dashed line in Fig. 4) is produced for $m_{\mathcal{H}^0} = 63 \text{ GeV}$ of the benchmark set in eq. (15). Since $m_{\mathcal{H}^0} \simeq m_h/2$ for the benchmark

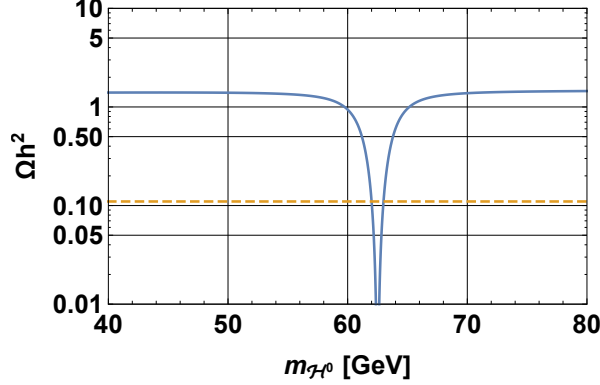


FIG. 4. The relic abundance of the scalar dark matter \mathcal{H}^0 in our model. The horizontal dashed line corresponds to $\Omega h^2 = 0.1186$ [3].

set, the h -mediation is the dominant annihilation process. Notice that the cross section for the self-annihilation in Fig. 3 is almost independent of $m_{\mathcal{H}^0}$ if $m_{\mathcal{H}^0}^2 \ll m_\psi^2$. Thus, even for a different value of $m_{\mathcal{H}^0}$, the constraint on $\Omega_{\text{DM}} h^2$ can be easily satisfied by adjusting the overall scale of Y_ψ^0 , which does not affect $\ell \rightarrow \ell' \gamma$ and $\mu \rightarrow \bar{e} e e$; the neutrino mass scale can be recovered to the appropriate value by changing μ' for example.

D. Strong First-Order Phase Transition

Baryon asymmetry of the Universe can be generated if the electroweak symmetry is broken via the strong first-order phase transition. Let us examine below whether the strong first-order phase transition can be achieved in our model or not. The effective potential V_{eff} at the one-loop level at the finite temperature T is given by the sum of the potential V_{tree} at the tree level, the one-loop correction ΔV at the zero temperature [20], the correction ΔV_T at the finite temperature [21] as follows:

$$V_{\text{eff}}(\varphi, T) = V_{\text{tree}}(\varphi) + \Delta V(\varphi) + \Delta V_T(\varphi, T) + \Delta V_{\text{ring}}, \quad (19)$$

$$V_{\text{tree}}(\varphi) = -\frac{m_h^2}{4}\varphi^2 + \frac{m_h^2}{8v^2}\varphi^4 + \frac{1}{2}A\varphi^2, \quad (20)$$

$$\Delta V(\varphi) = \frac{1}{64\pi^2} \sum_i n_i (-1)^{2s_i} \tilde{m}_i^4(\varphi) \left(\ln \frac{\tilde{m}_i^2(\varphi)}{Q^2} - c_i \right), \quad (21)$$

$$\Delta V_T(\varphi, T) = \frac{T^4}{2\pi^2} \sum_i n_i I_i \left(\frac{\tilde{m}_i^2(\varphi)}{T^2} \right), \quad (22)$$

where φ is the order parameter for the electroweak symmetry breaking, n_i denotes the degree of freedom for the particle i ($= t, W^\pm, Z, \gamma$, and scalar bosons), s_i is the spin. The field-

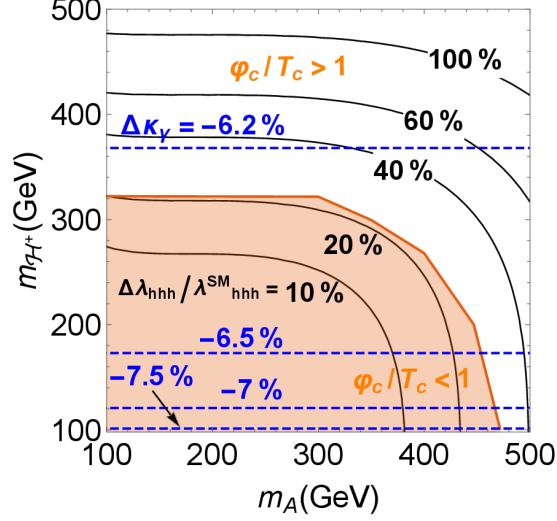


FIG. 5. In the white region, our model satisfies the condition $\varphi_c/T_c \gtrsim 1$ for the strong first-order phase transition, which is required for the electroweak baryogenesis scenario. Solid lines are contours of the deviation $\Delta\lambda_{hhh}/\lambda_{hhh}^{\text{SM}}$ of λ_{hhh} from the SM value $\lambda_{hhh}^{\text{SM}}$. Dashed lines show contours of the deviation $\Delta\kappa_\gamma$ of $\Gamma(h \rightarrow \gamma\gamma)$ from the SM value.

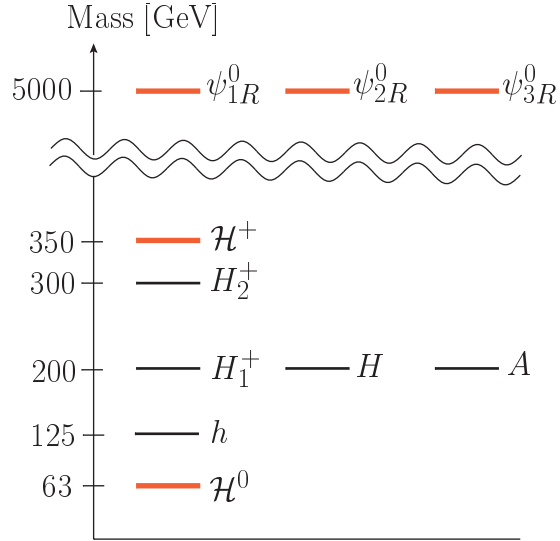


FIG. 6. Mass spectrum of h and new particles for the benchmark values in eqs. (15) and (18) with $m_A = 200$ GeV. Red bold bars show masses of Z_2 -odd particles.

dependent masses $\tilde{m}_i(\varphi)$ are shown in Appendix C. Contributions from the ring diagrams [22] are taken into account by replacing $\tilde{m}_i(\varphi)$ with $\tilde{m}_i(\varphi, T)$ at a finite temperature T , which are given in Appendix D. The constant c_i is $3/2$ for fermions and scalar bosons while it is $5/6$

for gauge bosons. The counter term A and the renormalization scale Q can be determined by renormalization conditions $\partial V_{\text{eff}}(\varphi, 0)/\partial\varphi|_{\varphi=v} = 0$ and $\partial^2 V_{\text{eff}}(\varphi, 0)/\partial\varphi^2|_{\varphi=v} = m_h^2$, where the infrared diverging $\ln \tilde{m}_i^2(v)$ of the Nambu-Goldstone bosons ($i = G^0, G^\pm$) are replaced with $\text{Re} \int_0^1 dx \ln\{-x(1-x)m_h^2\}$ [23]. The distribution functions are given by $I_i(\alpha^2) = \int_0^\infty dx x^2 \ln\{1 \mp \exp(-\sqrt{x^2 + \alpha^2})\}$, where the minus sign is for bosons and the plus sign is for fermions [21]. The critical temperature T_c and the critical value φ_c (φ at T_c) are obtained with $V_{\text{eff}}(\varphi_c, T_c) = 0$ and $\partial V_{\text{eff}}(\varphi, T_c)/\partial\varphi|_{\varphi=\varphi_c} = 0$. Then, $\varphi_c/T_c \gtrsim 1$ is required for the strong first-order phase transition [8]. It is shown in Fig. 5 that the condition is satisfied in the white region ($m_A \gtrsim 470$ GeV and $m_{\mathcal{H}^\pm} \gtrsim 300$ GeV). By taking $m_A = 200$ GeV as a benchmark value together with values in eqs. (15) and (18), the mass spectrum of scalar bosons and ψ_R^0 are presented in Fig. 6.

III. PHENOMENOLOGY

The Yukawa interaction with Y_ψ^+ causes $\ell \rightarrow \ell'\gamma$ via the $\mathcal{H}^+ - \psi_R^0$ loop. The branching ratio is calculated as

$$\text{BR}(\ell \rightarrow \ell'\gamma) = \frac{3\alpha_{\text{EM}}}{64\pi G_F^2 m_{\mathcal{H}^+}^4} \left| (Y_\psi^+ (Y_\psi^+)^\dagger)_{\ell\ell'} F_2\left(\frac{m_\psi^2}{m_{\mathcal{H}^+}^2}\right) \right|^2 \text{BR}(\ell \rightarrow e\nu\bar{\nu}), \quad (23)$$

where α_{EM} denotes the fine structure constant, G_F is the Fermi coupling constant, and $F_2(x) \equiv (1 - 6x + 3x^2 + 2x^3 - 6x^2 \ln x)/\{6(1-x)^4\}$. The benchmark set in eq. (15) result in $\text{BR}(\mu \rightarrow e\gamma) = 5.2 \times 10^{-14}$, $\text{BR}(\tau \rightarrow e\gamma) = 8.8 \times 10^{-15}$ and $\text{BR}(\tau \rightarrow \mu\gamma) = 8.8 \times 10^{-15}$, which satisfy current experimental bounds $\text{BR}(\mu \rightarrow e\gamma) < 4.2 \times 10^{-13}$ [24], $\text{BR}(\tau \rightarrow e\gamma) < 3.3 \times 10^{-8}$ [25] and $\text{BR}(\tau \rightarrow \mu\gamma) < 4.4 \times 10^{-8}$ [25]. The benchmark value for $\mu \rightarrow e\gamma$ is close to the expected sensitivity $\text{BR}(\mu \rightarrow e\gamma) = 6 \times 10^{-14}$ at the future MEG-II experiment [26] while benchmark values for $\tau \rightarrow \ell\gamma$ are too small to be measured.

The Yukawa interaction with Y_ψ^+ causes also $\mu \rightarrow \bar{e}ee$. Ignoring contributions of penguin diagrams because of constraints for $\ell \rightarrow \ell'\gamma$, the branching ratio for $\mu \rightarrow \bar{e}ee$ via box diagrams is given by

$$\begin{aligned} \text{BR}(\mu \rightarrow \bar{e}ee) = & \frac{1}{4G_F^2} \left| \sum_{a,b} (Y_\psi^+)_{ea}^* (Y_\psi^+)_{ae}^T (Y_\psi^+)_{eb}^* (Y_\psi^+)_{b\mu}^T (I_1^{\text{box}})_{ba} \right. \\ & \left. + \frac{1}{2} \sum_{a,b} (Y_\psi^+)_{ea}^* (Y_\psi^+)_{ae}^\dagger (Y_\psi^+)_{\mu b} (Y_\psi^+)_{be}^T m_{\psi_b} m_{\psi_a} (I_2^{\text{box}})_{ba} \right|^2, \quad (24) \end{aligned}$$

where formulae of loop functions $(I_1^{\text{box}})_{ba}$ and $(I_2^{\text{box}})_{ba}$ are shown in Appendix A. The experimental constraint $\text{BR}(\mu \rightarrow \bar{e}ee) < 1.0 \times 10^{-12}$ [27] is satisfied by the benchmark set in eq. (15), which gives $\text{BR}(\mu \rightarrow \bar{e}ee) = 1.0 \times 10^{-13}$. The benchmark value can be measured at the future Mu3e experiment, whose expected sensitivity is $\text{BR}(\mu \rightarrow \bar{e}ee) \sim 10^{-16}$ [28].

Although coupling constants $G_{\ell\ell'}$ for decays $\ell \rightarrow \ell'\nu\bar{\nu}$ are universal in the SM such that $G_{\ell\ell'} = G_F$, they can be different from each other due to contributions of new particles. The prediction $G_{\tau e}^2/G_F^2 \simeq G_{\tau\mu}^2/G_F^2 \lesssim 1$ is obtained for the Group-V in Ref. [10] by concentrating on the matrix structure of the neutrino mass matrix. In our explicit model, which belongs to the Group-V in Ref. [10], we can calculate the size of the lepton universality violation. The benchmark set in eq. (15) results in $G_{\tau e}^2/G_F^2 - 1 \sim G_{\tau\mu}^2/G_F^2 - 1 \sim -1 \times 10^{-15}$. These values are consistent with experimental bounds, $G_{\tau e}^2/G_F^2 = 1.0029 \pm 0.0046$ [29], $G_{\tau\mu}^2/G_F^2 = 0.981 \pm 0.018$ [29], and $G_{\tau\mu}^2/G_{\tau e}^2 = 1.0036 \pm 0.0020$ [30]. Deviations of these benchmark values from unity seem to be too small so that they cannot be measured.

The spin-independent scattering cross section σ_{SI} of the dark matter \mathcal{H}^0 on a proton can be calculated with the following formulae:

$$\sigma_{\text{SI}} = \frac{m_p^2}{4\pi(m_{\mathcal{H}^0} + m_p)^2} f_p^2, \quad (25)$$

$$\frac{f_p}{m_p} = \sum_{q=u,d,s} f_{Tq}^{(p)} \frac{f_q}{m_q} + \frac{2}{27} f_{TG}^{(p)} \sum_{q=c,b,t} \frac{f_q}{m_q}, \quad f_{TG}^{(p)} = 1 - \sum_{q=u,d,s} f_{Tq}^{(p)}. \quad (26)$$

The coupling constant f_q of the effective interaction $f_q \mathcal{H}^0 \mathcal{H}^{0*} \bar{q}q$ in our model is given by

$$\begin{aligned} \frac{f_q}{m_q} = & \frac{\lambda_{\phi 1s0} \sin \alpha \cos \beta - \lambda_{\phi 2s0} \cos \alpha \sin \beta}{m_h^2} \frac{\cos \alpha}{\sin \beta} \\ & - \frac{\lambda_{\phi 1s0} \cos \alpha \cos \beta + \lambda_{\phi 2s0} \sin \alpha \sin \beta}{m_H^2} \frac{\sin \alpha}{\sin \beta}, \end{aligned} \quad (27)$$

where α is the mixing angle for ϕ_{1r}^0 and ϕ_{2r}^0 . We take $\sin(\beta - \alpha) = 1$, $f_{Tu}^{(p)} = 0.016$ and $f_{Td}^{(p)} = 0.011$ [31] for $f_{Ts}^{(p)} = 0$ allowed by a lattice QCD calculation [32] in addition to values in eqs. (15) and (18). Then, we obtain $\sigma_{\text{SI}} = 5.0 \times 10^{-47} \text{ cm}^2$, which satisfies the current bound ($\sigma_{\text{SI}} \lesssim 10^{-46} \text{ cm}^2$ for $m_{\text{DM}} \simeq 100 \text{ GeV}$) [33]. The benchmark value is in expected sensitivity regions of the LZ experiment [34] and the XENON1T experiment [35].

There are three charged scalar particles in this model, which can contribute to $h \rightarrow \gamma\gamma$. Contours of $\Delta\kappa_\gamma$ ($\equiv \kappa_\gamma - 1$), where $\kappa_\gamma \equiv (\Gamma(h \rightarrow \gamma\gamma)/\Gamma(h \rightarrow \gamma\gamma)_{\text{SM}})^{1/2}$, are presented in Fig. 5 with dashed lines. The combined analysis of data obtained in the ATLAS and the CMS collaborations shows $|\kappa_\gamma| = 0.90_{-0.09}^{+0.10}$ [36]. The expected precision is 2-5% when the

3000 fb⁻¹ integrated luminosity is accumulated at the LHC [37]. The precision at the ILC can be about 3% [38] if 2000 fb⁻¹ data with $\sqrt{s} = 250$ GeV, 200 fb⁻¹ data with $\sqrt{s} = 350$ GeV, and 4000 fb⁻¹ data with $\sqrt{s} = 500$ GeV are combined (the H-20 operating scenario [39]). New charged scalars may also contribute to $h \rightarrow \gamma Z$. In our model, negative deviations are predicted for the $h\gamma\gamma$ coupling in most of the parameter space. The deviations are expected to be detected in above the experiments.

The hhh coupling constant λ_{hhh} can be evaluated by using V_{eff} at the zero temperature as $\lambda_{hhh} = \partial^3 V_{\text{eff}}(\varphi, 0)/\partial\varphi^3|_{\varphi=v}$, where diverging contributions of the Nambu-Goldstone bosons are removed. The deviation $\Delta\lambda_{hhh}$ ($\equiv \lambda_{hhh} - \lambda_{hhh}^{\text{SM}}$) of λ_{hhh} in our model ($\theta_+ = 0$ for simplicity) from the SM value $\lambda_{hhh}^{\text{SM}}$ is shown in Fig. 5. For this benchmark point, we see that $\Delta\lambda_{hhh}/\lambda_{hhh}^{\text{SM}} \gtrsim 20\%$ indicates $\varphi_c/T_c \gtrsim 1$. The high-luminosity LHC with 3000 fb⁻¹ is expected to measure signal from the Higgs boson pair production with the 54% uncertainty [40]. Precision of the measurement of λ_{hhh} at the ILC can be 26% at $\sqrt{s} = 500$ GeV for the H-20 operating scenario and 10% at $\sqrt{s} = 1$ TeV with the 8000 fb⁻¹ data [41]. The electroweak baryogenesis scenario in our model can be tested by precise measurements of λ_{hhh} at these future experiments similarly to the case in a two Higgs doublet model [42].

The strongly first-order phase transition in the early Universe can also be tested by detecting the characteristic spectrum of gravitational waves (GWs) [43–49] at future space based GW interferometers such as LISA [50], DECIGO [51] and BBO [52]. In particular, it has been decided that LISA will start in relatively near future [50]. In Refs. [53, 54], discrimination of new physics models with strongly first-order phase transition has been discussed at LISA and DECIGO. The synergy of collider experiments and GW measurement has been discussed in Refs. [54, 55].

There are two Z_2 -even charged Higgs bosons H_1^+ and H_2^+ in our model. Since s_3^+ does not have the Yukawa interaction, both of H_1^+ and H_2^+ decay into fermions via Yukawa interactions for Φ_1 or Φ_2 through the mixing with θ_+ . Since we take their Yukawa interactions to be the same as those in the type-X two Higgs double model, both of H_1^+ and H_2^+ decay into $\bar{\tau}\nu$ for the benchmark set in eq. (15). See e.g., Refs. [56–58] for the prospect of searches for H^+ in the the type-X two Higgs double model. If such two particles are discovered, our model might be preferable to the AKS model, which does not involve the second Z_2 -even charged Higgs boson.

IV. CONCLUSIONS

In this letter, we have proposed a model for generating tiny masses of Dirac neutrinos, where three right-handed neutrinos ν_{iR} are introduced to the SM with the lepton number conservation. Although Dirac neutrino masses at the tree level are forbidden by a softly broken Z_2 symmetry in order to avoid unnaturally small coupling constants, they are generated at the two-loop level, where neutrino masses are naturally suppressed. We have found a benchmark set of parameter values, which is consistent with neutrino oscillation data, constraints on charged lepton flavor violations ($\ell \rightarrow \ell' \gamma$ and $\mu \rightarrow \bar{e} e e$) and the violation of the lepton universality ($\ell \rightarrow \ell' \nu \bar{\nu}$). Masses of new particles can be less than the TeV-scale which can be probed at the current and future collider experiments, and unnaturally small coupling constants are not required. For the benchmark set, the dark matter candidate is the complex scalar \mathcal{H}^0 stabilized by the unbroken Z_2 symmetry, which is not imposed by hand but arises due to assignments of conserving lepton numbers to new fields. We have shown that the abundance and the spin-independent scattering cross section of the dark matter for the benchmark set are consistent with experimental constraints. In addition, the second $SU(2)_L$ -doublet scalar field can provide the source of the CP violation in the scalar potential in principle. It has been shown that the strong first-order phase transition for the electroweak symmetry breaking can be realized in our model as required for the electroweak baryogenesis scenario. Then, the deviation of the coupling constant for the hhh interaction from the value in the SM is more than about 20%, which can be tested at the future linear collider. Notice that Z_2 -odd fields (including the dark matter candidate) and the second $SU(2)_L$ -doublet scalar field (preferred for the electroweak baryogenesis) in our model are essential to generate neutrino masses. If one of them is removed from our model, neutrino masses are not generated. Therefore, our model can be a simultaneous solution for three problems, namely non-zero neutrino masses, the dark matter candidate, and the baryon asymmetry of the Universe.

ACKNOWLEDGMENTS

This work was supported, in part, by Grant-in-Aid for Scientific Research on Innovative Areas, the Ministry of Education, Culture, Sports, Science and Technology, No. 16H06492,

and Grant H2020-MSCA-RISE-2014 no. 645722 (Non Minimal Higgs).

Appendix A: Loop Functions

The two-loop function $I_{\ell a}$ in eq. (11) is defined as

$$\begin{aligned}
I_{\ell a} &\equiv \int \frac{d^4 p}{(2\pi)^4} \int \frac{d^4 q}{(2\pi)^4} \frac{1}{p^2 - m_{H_1^+}^2} \frac{1}{p^2 - m_{H_2^+}^2} \frac{p^\mu}{p^2 - m_\ell^2} \frac{1}{q^2 - m_{\mathcal{H}^0}^2} \frac{q_\mu}{q^2 - m_{\psi_a}^2} \frac{1}{(p-q)^2 - m_{\mathcal{H}^+}^2} \\
&= \frac{1}{(4\pi)^4 (m_{H_2^+}^2 - m_{H_1^+}^2) (m_{\psi_a}^2 - m_{\mathcal{H}^0}^2)} \\
&\int_0^1 dx x \left[\frac{1}{m_\ell^2 - m_{H_2^+}^2} \left\{ f(m_\ell^2) - f(m_{H_2^+}^2) \right\} - \frac{1}{m_\ell^2 - m_{H_1^+}^2} \left\{ f(m_\ell^2) - f(m_{H_1^+}^2) \right\} \right], \quad (\text{A1})
\end{aligned}$$

where we used

$$f(m^2) \equiv m^4 \left\{ \text{Li}_2(z_1(m^2)) - \text{Li}_2(z_2(m^2)) \right\}, \quad (\text{A2})$$

$$z_1(m^2) \equiv 1 - \frac{1}{m^2 x(1-x)} \left\{ m_{\mathcal{H}^0}^2 + x(m_{\mathcal{H}^+}^2 - m_{\mathcal{H}^0}^2) \right\}, \quad (\text{A3})$$

$$z_2(m^2) \equiv 1 - \frac{1}{m^2 x(1-x)} \left\{ m_{\psi_a}^2 + x(m_{\mathcal{H}^+}^2 - m_{\psi_a}^2) \right\}, \quad (\text{A4})$$

$$\text{Li}_2(z) = - \int_0^z dt \frac{1}{t} \ln(1-t). \quad (\text{A5})$$

Ignoring m_ℓ , the function can be simplified as

$$I_{\ell a} = I_a \equiv \frac{1}{(4\pi)^4 (m_{H_2^+}^2 - m_{H_1^+}^2) (m_{\psi_a}^2 - m_{\mathcal{H}^0}^2)} \int_0^1 dx x \left[\frac{f(m_{H_2^+}^2)}{m_{H_2^+}^2} - \frac{f(m_{H_1^+}^2)}{m_{H_1^+}^2} \right]. \quad (\text{A6})$$

Loop functions for box diagrams for $\ell_4(p_4) \rightarrow \bar{\ell}_3(-p_3) \ell_2(-p_2) \ell_1(-p_1)$ are defined as

$$\begin{aligned}
(I_1^{\text{box}})_{ba} &\equiv \frac{i^4}{4} \int \frac{d^4 k}{(2\pi)^4} \frac{k^\mu}{k^2 - m_{\psi_b}^2} \frac{1}{(k+p_1)^2 - m_{\mathcal{H}^+}^2} \\
&\quad \times \frac{(k+p_1+p_3)_\mu}{(k+p_1+p_3)^2 - m_{\psi_a}^2} \frac{1}{(k+p_1+p_2+p_3)^2 - m_{\mathcal{H}^+}^2} \\
&\simeq -\frac{i}{4(4\pi)^2} \left[\frac{m_{\mathcal{H}^+}^2}{(m_{\psi_a}^2 - m_{\mathcal{H}^+}^2)(m_{\psi_b}^2 - m_{\mathcal{H}^+}^2)} + \frac{m_{\psi_a}^4}{(m_{\psi_b}^2 - m_{\psi_a}^2)(m_{\mathcal{H}^+}^2 - m_{\psi_a}^2)^2} \ln \frac{m_{\mathcal{H}^+}^2}{m_{\psi_a}^2} \right. \\
&\quad \left. + \frac{m_{\psi_b}^4}{(m_{\psi_a}^2 - m_{\psi_b}^2)(m_{\mathcal{H}^+}^2 - m_{\psi_b}^2)^2} \ln \frac{m_{\mathcal{H}^+}^2}{m_{\psi_b}^2} \right], \quad (\text{A7})
\end{aligned}$$

$$\begin{aligned}
(I_2^{\text{box}})_{ba} &\equiv i^4 \int \frac{d^4 k}{(2\pi)^4} \frac{1}{k^2 - m_{\psi_b}^2} \frac{1}{(k+p_3)^2 - m_{\mathcal{H}^+}^2} \\
&\quad \times \frac{1}{(k+p_1+p_3)^2 - m_{\psi_a}^2} \frac{1}{(k+p_1+p_2+p_3)^2 - m_{\mathcal{H}^+}^2}
\end{aligned}$$

$$\simeq -\frac{i}{(4\pi)^2} \left[\frac{1}{(m_{\psi_a}^2 - m_{\mathcal{H}^+}^2)(m_{\psi_b}^2 - m_{\mathcal{H}^+}^2)} + \frac{m_{\psi_a}^2}{(m_{\psi_b}^2 - m_{\psi_a}^2)(m_{\mathcal{H}^+}^2 - m_{\psi_a}^2)^2} \ln \frac{m_{\mathcal{H}^+}^2}{m_{\psi_a}^2} \right. \\ \left. + \frac{m_{\psi_b}^2}{(m_{\psi_a}^2 - m_{\psi_b}^2)(m_{\mathcal{H}^+}^2 - m_{\psi_b}^2)^2} \ln \frac{m_{\mathcal{H}^+}^2}{m_{\psi_b}^2} \right]. \quad (\text{A8})$$

For $m_\psi \equiv m_{\psi_a} = m_{\psi_b}$, these functions are simplified as

$$(I_1^{\text{box}})_{ba} \simeq -\frac{i}{4(4\pi)^2} \left\{ \frac{m_\psi^2 + m_{\mathcal{H}^+}^2}{(m_\psi^2 - m_{\mathcal{H}^+}^2)^2} + \frac{2m_\psi^2 m_{\mathcal{H}^+}^2}{(m_\psi^2 - m_{\mathcal{H}^+}^2)^3} \ln \frac{m_{\mathcal{H}^+}^2}{m_\psi^2} \right\}, \quad (\text{A9})$$

$$(I_2^{\text{box}})_{ba} \equiv -\frac{i}{(4\pi)^2} \left\{ \frac{2}{(m_\psi^2 - m_{\mathcal{H}^+}^2)^2} + \frac{m_\psi^2 + m_{\mathcal{H}^+}^2}{(m_\psi^2 - m_{\mathcal{H}^+}^2)^3} \ln \frac{m_{\mathcal{H}^+}^2}{m_\psi^2} \right\}. \quad (\text{A10})$$

Appendix B: Annihilation Cross Section

The scalar dark matter \mathcal{H}^0 can annihilate into $b\bar{b}$ via the tree-level diagram in Fig. 2(a).

We obtain

$$\sigma(\mathcal{H}^0 \mathcal{H}^{0*} \rightarrow h(H) \rightarrow b\bar{b}) v_{\text{rel}} \\ \simeq \frac{3m_b^2}{4\pi v_2^2} \left(1 - \frac{m_b^2}{m_{\mathcal{H}^0}^2}\right)^{\frac{3}{2}} \left| \frac{\lambda_{h\mathcal{H}^0\mathcal{H}^0} \cos \alpha}{4m_{\mathcal{H}^0}^2 - m_h^2 + im_h \Gamma_h} + \frac{\lambda_{H\mathcal{H}^0\mathcal{H}^0} \sin \alpha}{4m_{\mathcal{H}^0}^2 - m_H^2 + im_H \Gamma_H} \right|^2, \quad (\text{B1})$$

where

$$\begin{pmatrix} \lambda_{H\mathcal{H}^0\mathcal{H}^0} \\ \lambda_{h\mathcal{H}^0\mathcal{H}^0} \end{pmatrix} \equiv \begin{pmatrix} \cos \alpha & \sin \alpha \\ -\sin \alpha & \cos \alpha \end{pmatrix} \begin{pmatrix} \lambda_{\phi_{1s0}} v_1 \\ \lambda_{\phi_{2s0}} v_2 \end{pmatrix}. \quad (\text{B2})$$

We used $\Gamma_h = 4.07 \times 10^{-3} \text{ GeV}$ for the total width of the discovered Higgs boson ($m_h = 125 \text{ GeV}$), and the total width of H is calculated as

$$\Gamma_H = \frac{m_H m_b^2}{8\pi v^2} \xi_{Hd}^2 \left(1 - \frac{4m_b^2}{m_H^2}\right)^{3/2} + \frac{m_H m_\tau^2}{8\pi v^2} \xi_{H\ell}^2 \left(1 - \frac{4m_\tau^2}{m_H^2}\right)^{3/2}, \quad (\text{B3})$$

where we take $\xi_{Hd} = \sin \alpha / \sin \beta$ and $\xi_{H\ell} = \cos \alpha / \cos \beta$.

There is another tree-level diagram (Fig. 2(b)) mediated by ψ_R^0 with the Yukawa coupling matrix Y_ψ^0 . The cross section is calculated as

$$\sigma(\mathcal{H}^0 \mathcal{H}^{0*} \rightarrow \nu_R \bar{\nu}_R) v_{\text{rel}} \simeq \frac{m_{\mathcal{H}^0}^2 v_{\text{rel}}^2}{48\pi} \sum_{a,b} \frac{|(Y_\psi^{0\dagger} Y_\psi^0)_{ab}|^2}{\{m_{\mathcal{H}^0}^2 + m_{\psi_a}^2\} \{m_{\mathcal{H}^0}^2 + m_{\psi_b}^2\}}. \quad (\text{B4})$$

The annihilation into a pair of photons is possible via one-loop diagrams in Figs. 2(c)-(f) without using Yukawa interactions. Contributions of Figs. 2(e) and (f) are completely cancelled by each other, and then we have

$$\begin{aligned} & \sigma(\mathcal{H}^0 \mathcal{H}^{0*} \rightarrow \gamma\gamma) v_{\text{rel}} \\ & \simeq \frac{4\pi\alpha_{\text{EM}}^2}{(16\pi^2)^2 m_{\mathcal{H}^0}^2} \left[\sum_i (\mu'_{3i})^2 \left\{ \frac{2m_{H_i^+}^2 m_{\mathcal{H}^+}^2}{(m_{H_i^+}^2 - m_{\mathcal{H}^+}^2)^3} \ln \frac{m_{H_i^+}^2}{m_{\mathcal{H}^+}^2} - \frac{m_{H_i^+}^2 + m_{\mathcal{H}^+}^2}{(m_{H_i^+}^2 - m_{\mathcal{H}^+}^2)^2} \right\} \right]^2, \end{aligned} \quad (\text{B5})$$

where $\mu'_{31} \equiv \mu'_3 \sin \theta_+$ and $\mu'_{32} \equiv \mu'_3 \cos \theta_+$.

The annihilation into a pair of charged leptons can be caused not only by the tree-level diagram in Fig. 2(a) with the usual Yukawa interaction but also by the one-loop diagrams in Fig. 2(g) and 2(h) with new Yukawa coupling matrix Y_ψ^+ . We obtain

$$\sigma(\mathcal{H}^0 \mathcal{H}^{0*} \rightarrow \ell \bar{\ell}') v_{\text{rel}} \simeq \frac{1}{8\pi} \left\{ (m_\ell^2 + m_{\ell'}^2) |A_{\ell\ell'}|^2 + \frac{2}{3} m_{\mathcal{H}^0}^2 |(B_{\text{box}})_{\ell\ell'}|^2 v_{\text{rel}}^2 \right\}, \quad (\text{B6})$$

where the following formulae are used:

$$A_{\ell\ell'} \equiv (A_{\text{tree}})_\ell \delta_{\ell\ell'} + (A_{\text{tri}})_{\ell\ell'} + (A_{\text{box}})_{\ell\ell'}, \quad (\text{B7})$$

$$(A_{\text{tree}})_\ell \equiv \frac{i}{v_1} \left\{ \frac{\lambda_{h\mathcal{H}^0\mathcal{H}^0} \sin \alpha}{4m_{\mathcal{H}^0}^2 - m_h^2 + im_h\Gamma_h} - \frac{\lambda_{H\mathcal{H}^0\mathcal{H}^0} \cos \alpha}{4m_{\mathcal{H}^0}^2 - m_H^2 + im_H\Gamma_H} \right\}, \quad (\text{B8})$$

$$(A_{\text{tri}})_{\ell\ell'} \equiv -\frac{i\lambda_{s0s2}}{2(4\pi)^2} \sum_a (Y_\psi^+)_{\ell a}^* (Y_\psi^+)_{a\ell'}^T \left\{ \frac{m_{\psi_a}^4}{(m_{\mathcal{H}^+}^2 - m_{\psi_a}^2)^3} \ln \frac{m_{\mathcal{H}^+}^2}{m_{\psi_a}^2} + \frac{m_{\mathcal{H}^+}^2 - 3m_{\psi_a}^2}{2(m_{\mathcal{H}^+}^2 - m_{\psi_a}^2)^2} \right\}, \quad (\text{B9})$$

$$\begin{aligned} (A_{\text{box}})_{\ell\ell'} \equiv & \frac{i}{(4\pi)^2} \sum_{a,i} (Y_\psi^+)_{\ell a}^* (Y_\psi^+)_{a\ell'}^T (\mu'_{3i})^2 \\ & \left\{ -\frac{m_{H_i^+}^2 (m_{H^+}^2 - 2m_{\psi_a}^2)}{4(m_{\mathcal{H}^+}^2 - m_{H_i^+}^2)^2 (m_{\psi_a}^2 - m_{H_i^+}^2)^2} \ln \frac{m_{H_i^+}^2}{m_{\psi_a}^2} \right. \\ & - \frac{2m_{\psi_a}^4 m_{H_i^+}^2 - 3m_{\psi_a}^2 m_{\mathcal{H}^+}^4 + m_{\mathcal{H}^+}^6}{4(m_{\psi_a}^2 - m_{\mathcal{H}^+}^2)^3 (m_{H_i^+}^2 - m_{\mathcal{H}^+}^2)^2} \ln \frac{m_{\mathcal{H}^+}^2}{m_{\psi_a}^2} \\ & \left. + \frac{2m_{\psi_a}^4 - 3m_{\psi_a}^2 m_{H_i^+}^2 + m_{\mathcal{H}^+}^2 m_{H_i^+}^2}{4(m_{\psi_a}^2 - m_{\mathcal{H}^+}^2)^2 (m_{\psi_a}^2 - m_{H_i^+}^2) (m_{\mathcal{H}^+}^2 - m_{H_i^+}^2)} \right\}, \end{aligned} \quad (\text{B10})$$

$$\begin{aligned}
(B_{\text{box}})_{\ell\ell'} \equiv & \frac{i}{(4\pi)^2} \sum_{a,i} (Y_{\psi^+}^*)_{\ell a} (Y_{\psi^+}^T)_{a\ell'} (\mu'_{3i})^2 \\
& \left\{ -\frac{m_{H_i^+}^2 (-2m_{\psi_a}^2 m_{\mathcal{H}^+}^2 + m_{\mathcal{H}^+}^2 m_{H_i^+}^2 + m_{H_i^+}^4)}{4(m_{\psi_a}^2 - m_{H_i^+}^2)^2 (m_{\mathcal{H}^+}^2 - m_{H_i^+}^2)^3} \ln \frac{m_{H_i^+}^2}{m_{\psi_a}^2} \right. \\
& - \frac{m_{\mathcal{H}^+}^2 (-2m_{\psi_a}^2 m_{H_i^+}^2 + m_{\mathcal{H}^+}^2 m_{H_i^+}^2 + m_{\mathcal{H}^+}^4)}{4(m_{\psi_a}^2 - m_{\mathcal{H}^+}^2)^2 (m_{H_i^+}^2 - m_{\mathcal{H}^+}^2)^3} \ln \frac{m_{\mathcal{H}^+}^2}{m_{\psi_a}^2} \\
& \left. + \frac{m_{\psi_a}^2 (m_{\mathcal{H}^+}^2 + m_{H_i^+}^2) - 2m_{\mathcal{H}^+}^2 m_{H_i^+}^2}{4(m_{\psi_a}^2 - m_{\mathcal{H}^+}^2)(m_{\psi_a}^2 - m_{H_i^+}^2)(m_{\mathcal{H}^+}^2 - m_{H_i^+}^2)^2} \right\} \quad (\text{B11})
\end{aligned}$$

The self-annihilation of \mathcal{H}^0 into two $\overline{\nu}_R$ is also possible via the diagram in Fig. 3, which results in

$$\sigma(\mathcal{H}^0 \mathcal{H}^0 \rightarrow \overline{\nu}_R \overline{\nu}_R) v_{\text{rel}} \simeq \sum_{a,b} \frac{\left\{ (Y_{\psi^0}^{\dagger} Y_{\psi^0})_{ab} \right\}^2 m_{\psi_a} m_{\psi_b}}{4\pi (m_{\mathcal{H}^0}^2 + m_{\psi_a}^2)(m_{\mathcal{H}^0}^2 + m_{\psi_b}^2)}. \quad (\text{B12})$$

Appendix C: Field-Dependent Masses

Field-dependent masses $\tilde{m}_i(\varphi)$ of particles i are given by

$$\tilde{m}_h^2(\varphi) = \frac{3m_h^2}{2} \left(\frac{\varphi^2}{v^2} - \frac{1}{3} \right), \quad (\text{C1})$$

$$\tilde{m}_{G^0}^2(\varphi) = \tilde{m}_{G^\pm}^2(\varphi) = \frac{m_h^2}{2} \left(\frac{\varphi^2}{v^2} - 1 \right), \quad (\text{C2})$$

$$\tilde{m}_H^2(\varphi) = \left(m_H^2 - \frac{2m_{12}^2}{\sin(2\beta)} + \frac{m_h^2}{2} \right) \frac{\varphi^2}{v^2} + \left(\frac{2m_{12}^2}{\sin(2\beta)} - \frac{m_h^2}{2} \right), \quad (\text{C3})$$

$$\tilde{m}_A^2(\varphi) = \left(m_A^2 - \frac{2m_{12}^2}{\sin(2\beta)} + \frac{m_h^2}{2} \right) \frac{\varphi^2}{v^2} + \left(\frac{2m_{12}^2}{\sin(2\beta)} - \frac{m_h^2}{2} \right), \quad (\text{C4})$$

$$\tilde{m}_{\mathcal{H}^0}^2(\varphi) = (m_{\mathcal{H}^0}^2 - m_{s0}^2) \frac{\varphi^2}{v^2} + m_{s0}^2, \quad (\text{C5})$$

$$\tilde{m}_{\mathcal{H}^\pm}^2(\varphi) = (m_{\mathcal{H}^\pm}^2 - m_{s2}^2) \frac{\varphi^2}{v^2} + m_{s2}^2, \quad (\text{C6})$$

$$\tilde{m}_{H_1^\pm}^2(\varphi) = \frac{1}{2} \left\{ (\widetilde{M}_{H^+}^{\prime 2})_{11} + (\widetilde{M}_{H^+}^{\prime 2})_{22} - \sqrt{((\widetilde{M}_{H^+}^{\prime 2})_{22} - (\widetilde{M}_{H^+}^{\prime 2})_{11})^2 - 4(\widetilde{M}_{H^+}^{\prime 2})_{12}^2} \right\}, \quad (\text{C7})$$

$$\tilde{m}_{H_2^\pm}^2(\varphi) = \frac{1}{2} \left\{ (\widetilde{M}_{H^+}^{\prime 2})_{11} + (\widetilde{M}_{H^+}^{\prime 2})_{22} + \sqrt{((\widetilde{M}_{H^+}^{\prime 2})_{22} - (\widetilde{M}_{H^+}^{\prime 2})_{11})^2 - 4(\widetilde{M}_{H^+}^{\prime 2})_{12}^2} \right\}, \quad (\text{C8})$$

$$(\widetilde{M}_{H^+}^{\prime 2})_{11} = \left(m_{H_1^\pm}^2 \cos^2 \theta_+ + m_{H_2^\pm}^2 \sin^2 \theta_+ - \frac{2m_{12}^2}{\sin(2\beta)} + \frac{m_h^2}{2} \right) \frac{\varphi^2}{v^2} + \frac{2m_{12}^2}{\sin(2\beta)} - \frac{m_h^2}{2}, \quad (\text{C9})$$

$$(\widetilde{M}_{H^+}^{\prime 2})_{22} = \left(m_{H_1^\pm}^2 \sin^2 \theta_+ + m_{H_2^\pm}^2 \cos^2 \theta_+ - m_{s3}^2 \right) \frac{\varphi^2}{v^2} + m_{s3}^2, \quad (\text{C10})$$

$$(\widetilde{M}_{H^+}^{\prime 2})_{12} = \frac{\varphi}{2v} (m_{H_1^\pm}^2 - m_{H_2^\pm}^2) \sin(2\theta_+), \quad (\text{C11})$$

$$\tilde{m}_t^2(\varphi) = m_t^2 \frac{\varphi^2}{v^2}, \quad (\text{C12})$$

$$\tilde{m}_W^2(\varphi) = m_W^2 \frac{\varphi^2}{v^2}, \quad (\text{C13})$$

$$\tilde{m}_Z^2(\varphi) = m_Z^2 \frac{\varphi^2}{v^2}, \quad (\text{C14})$$

where we take $2m_{12}^2/\sin(2\beta) = (200 \text{ GeV})^2$, $m_{s2}^2 = 0$, and $m_{s3}^2 = (300 \text{ GeV})^2$. Notice that $m_{s0}^2 \simeq (61 \text{ GeV})^2$ is obtained with eqs. (4), (15), and (18).

Appendix D: Thermal Masses

Field-dependent masses are thermally corrected at a finite temperature by contributions of ring diagrams. We only focus on the leading terms of $\mathcal{O}(T^2)$ [22, 59]. At a finite temperature T , field-dependent masses $\tilde{m}_i(\varphi, T)$ of Z_2 -odd scalar particles ($i = \mathcal{H}^0, \mathcal{H}^\pm$) are given by

$$\tilde{m}_{\mathcal{H}^0}^2(\varphi, T) = \tilde{m}_{\mathcal{H}^0}^2(\varphi) + \frac{T^2}{12} \left\{ 2(\lambda_{\phi 1s0} + \lambda_{\phi 2s0}) + 4\lambda_{s0} + \lambda_{s0s2} + \lambda_{s0s3} \right\}, \quad (\text{D1})$$

$$\tilde{m}_{\mathcal{H}^\pm}^2(\varphi, T) = \tilde{m}_{\mathcal{H}^\pm}^2(\varphi) + \frac{T^2}{12} \left\{ 2(\lambda_{\phi 1s2} + \lambda_{\phi 2s2}) + 4\lambda_{s2} + \lambda_{s0s2} + \lambda_{s2s3} \right\}. \quad (\text{D2})$$

Field-dependent squared masses $\tilde{m}_i^2(\varphi, T)$ of Z_2 -even scalar particles ($i = h, H, G^0, A^0, G^\pm, H_1^\pm$, and H_2^\pm) at a finite temperature are given as eigenvalues of the following matrices ($\tilde{M}_H^2(\varphi, T)$ for CP-even ones, $\tilde{M}_A^2(\varphi, T)$ for CP-odd ones, and $\tilde{M}_{H^\pm}^2(\varphi, T)$ for charged ones)

$$\tilde{M}_H^2(\varphi, T) = \begin{pmatrix} \cos \beta & -\sin \beta \\ \sin \beta & \cos \beta \end{pmatrix} \begin{pmatrix} \tilde{m}_h^2(\varphi) & 0 \\ 0 & \tilde{m}_H^2(\varphi) \end{pmatrix} \begin{pmatrix} \cos \beta & \sin \beta \\ -\sin \beta & \cos \beta \end{pmatrix} + \begin{pmatrix} \Pi_{\phi_1}(T) & 0 \\ 0 & \Pi_{\phi_2}(T) \end{pmatrix}, \quad (\text{D3})$$

$$\tilde{M}_A^2(\varphi, T) = \begin{pmatrix} \cos \beta & -\sin \beta \\ \sin \beta & \cos \beta \end{pmatrix} \begin{pmatrix} \tilde{m}_{G^0}^2(\varphi) & 0 \\ 0 & \tilde{m}_A^2(\varphi) \end{pmatrix} \begin{pmatrix} \cos \beta & \sin \beta \\ -\sin \beta & \cos \beta \end{pmatrix} + \begin{pmatrix} \Pi_{\phi_1}(T) & 0 \\ 0 & \Pi_{\phi_2}(T) \end{pmatrix}, \quad (\text{D4})$$

$$\begin{aligned} \widetilde{M}_{H^+}^2(\varphi, T) = & \begin{pmatrix} \cos \beta & -\sin \beta \cos \theta_+ & \sin \beta \sin \theta_+ \\ \sin \beta & \cos \beta \cos \theta_+ & -\cos \beta \sin \theta_+ \\ 0 & \sin \theta_+ & \cos \theta_+ \end{pmatrix} \begin{pmatrix} \widetilde{m}_{G^+}^2(\varphi) & 0 & 0 \\ 0 & \widetilde{m}_{H_1^+}^2(\varphi) & 0 \\ 0 & 0 & \widetilde{m}_{H_2^+}^2(\varphi) \end{pmatrix} \\ & + \begin{pmatrix} \cos \beta & \sin \beta & 0 \\ -\sin \beta \cos \theta_+ & \cos \beta \cos \theta_+ & \sin \theta_+ \\ \sin \beta \sin \theta_+ & -\cos \beta \sin \theta_+ & \cos \theta_+ \end{pmatrix} + \begin{pmatrix} \Pi_{\phi_1}(T) & 0 & 0 \\ 0 & \Pi_{\phi_2}(T) & 0 \\ 0 & 0 & \Pi_{s_3^+}(T) \end{pmatrix}, \end{aligned} \quad (\text{D5})$$

where thermal masses are given by

$$\Pi_{\phi_1}(T) = T^2 \left\{ \frac{3g^2 + g'^2}{16} + \frac{y_\tau}{12} + \frac{1}{12} (3\lambda_1 + 2\lambda_3 + \lambda_4 + \lambda_{\phi_1 s_0} + \lambda_{\phi_1 s_2} + \lambda_{\phi_1 s_3}) \right\}, \quad (\text{D6})$$

$$\Pi_{\phi_2}(T) = T^2 \left\{ \frac{3g^2 + g'^2}{16} + \frac{y_t + y_b}{12} + \frac{1}{12} (3\lambda_2 + 2\lambda_3 + \lambda_4 + \lambda_{\phi_2 s_0} + \lambda_{\phi_2 s_2} + \lambda_{\phi_2 s_3}) \right\}, \quad (\text{D7})$$

$$\Pi_{s_3^+}(T) = \frac{T^2}{12} \left\{ 2(\lambda_{\phi_1 s_3} + \lambda_{\phi_2 s_3}) + 4\lambda_{s_3} + \lambda_{s_0 s_3} + \lambda_{s_2 s_3} \right\}. \quad (\text{D8})$$

The field-dependent mass $\widetilde{m}_W^2(\varphi, T)$ of the W boson is given by

$$\widetilde{m}_W^2(\varphi, T) = \widetilde{m}_W^2(\varphi) + 2g^2 T^2. \quad (\text{D9})$$

On the other hand, $\widetilde{m}_i^2(\varphi, T)$ for $i = Z$ and γ are obtained as eigenvalues of the following matrix:

$$\widetilde{M}_Z^2(\varphi, T) = \frac{\varphi^2}{4} \begin{pmatrix} g^2 & gg' \\ gg' & g'^2 \end{pmatrix} + 2T^2 \begin{pmatrix} g^2 & 0 \\ 0 & g'^2 \end{pmatrix}. \quad (\text{D10})$$

In the calculation for φ_c/T_c , we take $\lambda_{\phi_1 s_0} = 0.02$ and $\lambda_{\phi_2 s_0} = 0.005$ in eq. (18) as well as $\lambda_{\phi_1 s_2} = \lambda_{\phi_1 s_3} = 0.1$, $\lambda_{s_0 s_2} = \lambda_{s_0 s_3} = \lambda_{s_2 s_3} = 0$, and $\lambda_{s_0} = \lambda_{s_2} = \lambda_{s_3} = 0$. The other coupling constants in the scalar potential V are determined by

$$\lambda_1 = \frac{1}{v^2 \cos^2 \beta} (-m_{12}^2 \tan \beta + m_h^2 \sin^2 \alpha + m_H^2 \cos^2 \alpha), \quad (\text{D11})$$

$$\lambda_2 = \frac{1}{v^2 \sin^2 \beta} (-m_{12}^2 \cot \beta + m_h^2 \cos^2 \alpha + m_H^2 \sin^2 \alpha), \quad (\text{D12})$$

$$\lambda_3 = \frac{1}{v^2} \left\{ -\frac{2m_{12}^2}{\sin(2\beta)} + \frac{\sin(2\alpha)}{\sin(2\beta)} (m_H^2 - m_h^2) + 2m_{H_1^+}^2 \cos^2 \theta_+ + 2m_{H_2^+}^2 \sin^2 \theta_+ \right\}, \quad (\text{D13})$$

$$\lambda_4 = \frac{1}{v^2} \left(\frac{2m_{12}^2}{\sin(2\beta)} + m_A^2 - 2m_{H_1^+}^2 \cos^2 \theta_+ - 2m_{H_2^+}^2 \sin^2 \theta_+ \right), \quad (\text{D14})$$

$$\lambda_5 = \frac{1}{v^2} \left(\frac{2m_{12}^2}{\sin(2\beta)} - m_A^2 \right), \quad (\text{D15})$$

$$\lambda_{\phi 2s2} = \frac{1}{v^2 \sin^2 \beta} (2m_{H^\pm}^2 - 2m_{s2}^2 - \lambda_{\phi 1s2} v^2 \cos^2 \beta), \quad (\text{D16})$$

$$\lambda_{\phi 2s3} = \frac{1}{v^2 \sin^2 \beta} \left(2m_{H_1^\pm}^2 \sin^2 \theta_+ + 2m_{H_2^\pm}^2 \cos^2 \theta_+ - 2m_{s3}^2 - \lambda_{\phi 1s3} v^2 \cos^2 \beta \right). \quad (\text{D17})$$

These values at the benchmark point are $\lambda_1 \simeq 0.26$, $\lambda_2 \simeq 0.26$, $\lambda_3 \simeq 0.27$, $\lambda_4 \simeq -0.017$, $\lambda_5 = 0$, $\lambda_{\phi 2s2} \simeq 4.5$, and $\lambda_{\phi 2s3} \simeq -0.030$.

-
- [1] G. Aad *et al.* [ATLAS Collaboration], Phys. Lett. B **716**, 1 (2013); S. Chatrchyan *et al.* [CMS Collaboration], Phys. Lett. B **716**, 30 (2012).
- [2] Y. Fukuda *et al.* [Super-Kamiokande Collaboration], Phys. Rev. Lett. **81**, 1562 (1998); Q. R. Ahmad *et al.* [SNO Collaboration], Phys. Rev. Lett. **89**, 011301 (2002).
- [3] P. A. R. Ade *et al.* [Planck Collaboration], Astron. Astrophys. **594**, A13 (2016).
- [4] P. Minkowski, Phys. Lett. B **67**, 421 (1977); T. Yanagida, Conf. Proc. C **7902131**, 95 (1979); Prog. Theor. Phys. **64**, 1103 (1980); M. Gell-Mann, P. Ramond and R. Slansky, Conf. Proc. C **790927**, 315 (1979); R. N. Mohapatra and G. Senjanovic, Phys. Rev. Lett. **44**, 912 (1980); J. Schechter and J. W. F. Valle, Phys. Rev. D **22**, 2227 (1980).
- [5] M. Fukugita and T. Yanagida, Phys. Lett. B **174**, 45 (1986).
- [6] E. Ma, Phys. Rev. D **73**, 077301 (2006); J. Kubo, E. Ma and D. Suematsu, Phys. Lett. B **642**, 18 (2006).
- [7] M. Aoki, S. Kanemura and O. Seto, Phys. Rev. Lett. **102**, 051805 (2009); Phys. Rev. D **80**, 033007 (2009); M. Aoki, S. Kanemura and K. Yagyu, Phys. Rev. D **83**, 075016 (2011).
- [8] V. A. Kuzmin, V. A. Rubakov and M. E. Shaposhnikov, Phys. Lett. **155B**, 36 (1985).
- [9] S. Kanemura and H. Sugiyama, Phys. Lett. B **753**, 161 (2016).
- [10] S. Kanemura, K. Sakurai and H. Sugiyama, Phys. Lett. B **758**, 465 (2016).
- [11] M. Aoki, S. Kanemura, K. Tsumura and K. Yagyu, Phys. Rev. D **80**, 015017 (2009).
- [12] V. D. Barger, J. L. Hewett and R. J. N. Phillips, Phys. Rev. D **41**, 3421 (1990).
- [13] Y. Grossman, Nucl. Phys. B **426**, 355 (1994).
- [14] A. G. Akeroyd and W. J. Stirling, Nucl. Phys. B **447**, 3 (1995); A. G. Akeroyd, Phys. Lett. B **377**, 95 (1996); J. Phys. G **24**, 1983 (1998).
- [15] Z. Maki, M. Nakagawa and S. Sakata, Prog. Theor. Phys. **28**, 870 (1962).
- [16] K. Abe *et al.* [T2K Collaboration], Phys. Rev. D **91**, no. 7, 072010 (2015).

- [17] F. P. An *et al.* [Daya Bay Collaboration], arXiv:1610.04802 [hep-ex].
- [18] B. Aharmim *et al.* [SNO Collaboration], Phys. Rev. C **88**, no. 2, 025501 (2013).
- [19] E. W. Kolb and M. S. Turner, “The Early Universe,” Front. Phys. **69**, 1 (1990).
- [20] L. Di Luzio and L. Mihaila, JHEP **1406**, 079 (2014).
- [21] L. Dolan and R. Jackiw, Phys. Rev. D **9**, 3320 (1974).
- [22] M. E. Carrington, Phys. Rev. D **45**, 2933 (1992).
- [23] J. M. Cline and P. A. Lemieux, Phys. Rev. D **55**, 3873 (1997).
- [24] A. M. Baldini *et al.* [MEG Collaboration], Eur. Phys. J. C **76**, no. 8, 434 (2016).
- [25] B. Aubert *et al.* [BaBar Collaboration], Phys. Rev. Lett. **104**, 021802 (2010).
- [26] A. M. Baldini *et al.*, arXiv:1301.7225 [physics.ins-det].
- [27] U. Bellgardt *et al.* [SINDRUM Collaboration], Nucl. Phys. B **299**, 1 (1988).
- [28] A. Blondel *et al.*, arXiv:1301.6113 [physics.ins-det].
- [29] C. Patrignani *et al.* [Particle Data Group], Chin. Phys. C **40**, no. 10, 100001 (2016).
- [30] B. Aubert *et al.* [BaBar Collaboration], Phys. Rev. Lett. **105**, 051602 (2010).
- [31] J. R. Ellis, K. A. Olive and C. Savage, Phys. Rev. D **77**, 065026 (2008).
- [32] H. Ohki *et al.*, Phys. Rev. D **78**, 054502 (2008); PoS LAT **2009**, 124 (2009).
- [33] D. S. Akerib *et al.* [LUX Collaboration], Phys. Rev. Lett. **118**, no. 2, 021303 (2017).
- [34] D. S. Akerib *et al.* [LZ Collaboration], arXiv:1509.02910 [physics.ins-det].
- [35] E. Aprile *et al.* [XENON Collaboration], JCAP **1604**, no. 04, 027 (2016).
- [36] G. Aad *et al.* [ATLAS and CMS Collaborations], JHEP **1608**, 045 (2016).
- [37] S. Dawson *et al.*, arXiv:1310.8361 [hep-ex].
- [38] K. Fujii *et al.*, arXiv:1506.05992 [hep-ex].
- [39] T. Barklow, J. Brau, K. Fujii, J. Gao, J. List, N. Walker and K. Yokoya, arXiv:1506.07830 [hep-ex].
- [40] CMS Collaboration [CMS Collaboration], CMS-PAS-FTR-15-002.
- [41] K. Fujii *et al.*, arXiv:1702.05333 [hep-ph].
- [42] S. Kanemura, Y. Okada and E. Senaha, Phys. Lett. B **606**, 361 (2005) doi:10.1016/j.physletb.2004.12.004 [hep-ph/0411354].
- [43] R. Apreda, M. Maggiore, A. Nicolis and A. Riotto, Nucl. Phys. B **631**, 342 (2002).
- [44] C. Grojean and G. Servant, Phys. Rev. D **75**, 043507 (2007).
- [45] J. R. Espinosa, T. Konstandin, J. M. No and M. Quiros, Phys. Rev. D **78**, 123528 (2008).

- [46] C. Caprini *et al.*, JCAP **1604**, no. 04, 001 (2016).
- [47] S. J. Huber, T. Konstandin, G. Nardini and I. Rues, JCAP **1603**, no. 03, 036 (2016).
- [48] M. Chala, G. Nardini and I. Sobolev, Phys. Rev. D **94**, no. 5, 055006 (2016).
- [49] A. Kobakhidze, A. Manning and J. Yue, arXiv:1607.00883 [hep-ph].
- [50] H. Audley *et al.*, arXiv:1702.00786 [astro-ph.IM]. See also <https://lisa.nasa.gov/>
- [51] S. Kawamura *et al.*, Class. Quant. Grav. **28**, 094011 (2011).
- [52] V. Corbin and N. J. Cornish, Class. Quant. Grav. **23**, 2435 (2006).
- [53] M. Kakizaki, S. Kanemura and T. Matsui, Phys. Rev. D **92**, no. 11, 115007 (2015).
- [54] K. Hashino, M. Kakizaki, S. Kanemura and T. Matsui, Phys. Rev. D **94**, no. 1, 015005 (2016).
- [55] K. Hashino, M. Kakizaki, S. Kanemura, P. Ko and T. Matsui, Phys. Lett. B **766**, 49 (2017).
- [56] S. Kanemura, K. Tsumura and H. Yokoya, Phys. Rev. D **85**, 095001 (2012).
- [57] S. Kanemura, H. Yokoya and Y. J. Zheng, Nucl. Phys. B **886**, 524 (2014).
- [58] S. Kanemura, K. Tsumura, K. Yagyu and H. Yokoya, Phys. Rev. D **90**, 075001 (2014).
- [59] L. Sagunski, DESY-THESIS-2016-023.